INT. J. CONTROL, 1993, VOL. 58, NO. 3, 555–586

Subspace model identification
Part 3. Analysis of the ordinary output-error state-space model identification algorithm

MICHEL VERHAEGEN†

The ordinary MOESP algorithm presented in the first part of this series of papers is analysed and extended in this paper. First, an analysis is made which proves that the asymptotic unbiasedness of the estimated state-space quadruple $[A_T, B_T, C_T, D]$ critically depends on the unbiased calculation of the column space of the extended observability matrix. Second, it is proved that the latter quantity can be calculated asymptotically unbiasedly only when the stochastic additive errors on the output quantity are zero-mean white noise. The extension of the ordinary MOESP scheme with instrumental variables increases the applicability of this scheme. Two types of instrumental variables are proposed: (1) based on past input measurements; and (2) based on reconstructed state quantities. The first type yields asymptotic unbiased estimates when the perturbation on the output quantity is an arbitrary zero-mean stochastic process independent of the error-free input. However, a detailed sensitivity analysis demonstrates that for the finite data-length case the calculations can become very sensitive; this occurs when the particular system at hand has dominant modes close to the unit circle. In the same sensitivity analysis it is shown that far more robust results can be obtained with the second type of instrumental variables when the true state quantities are used. A number of guidelines are derived from the given sensitivity analysis to obtain accurate reconstructed state quantities. Efficient numerical implementations are presented for both extensions of the ordinary MOESP scheme. The obtained insights are verified by means of two realistic simulation studies. The developed extensions and strategy in these studies demonstrate excellent performances in the treatment of both identification problems.

1. Introduction

In the third and final part of this series of papers, we analyse and extend the identification capabilities of the ordinary MOESP scheme. First, we study the asymptotic unbiasedness of the ordinary MOESP scheme for the simple identification problem stated in Part 2 (Verhaegen and Dewilde 1992 b). Second we extend the capabilities of the ordinary MOESP scheme to a realistic version of the global identification problem, stated in Part 1 (Verhaegen and Dewilde 1992 a), by incorporating instrumental variables in this scheme.

The realistic version of the open-loop global identification problem is stated next with the help of Fig. 1. As in Part 1 (Verhaegen and Dewilde 1992 a), we assume the different stochastic signals in the identification problem to be stationary, ergodic stochastic processes.

A realistic open-loop identification experiment and problem. *Apply* a computer-generated input sequence $u(k)$ via the necessary transducers to the

Received 7 February 1992. Revised 20 July 1992.

† Network Theory Section, Department of Electrical Engineering, Delft University of Technology, PO Box 4, NL-2600 GA Delft, The Netherlands.

0020-7179/93 $10.00 © 1993 Taylor & Francis Ltd

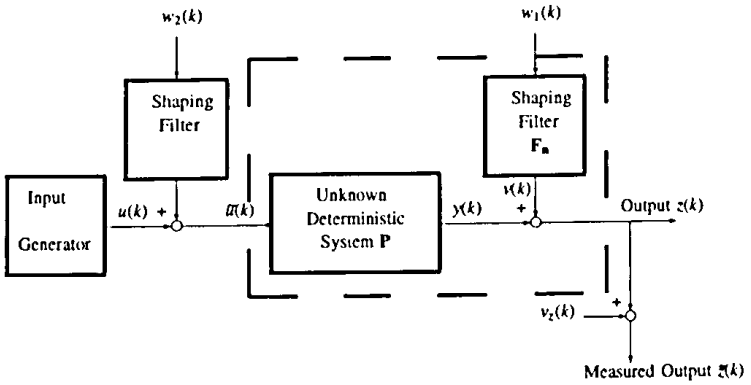

Figure 1. Block schematic view of a realistic system open-loop identification set-up.

linear time-invariant and finite dimensional (LTIFD) system, represented by the dashed box in Fig. 1. Owing to imperfect transducers, the actual input to the system $\tilde{u}(k)$ differs from the generated one. *Record* the output sequence $z(k)$. The measurement equipment used for that purpose further introduces the additive errors $v_z(k)$. *Assume* that the different zero-mean and additive transducer errors due to $w_2(k)$, modelling errors, due to $w_1(k)$ and measurement errors $v_z(k)$ are statistically independent of the generated input sequence $u(k)$. Then, the *task* is to approximate the input–output behaviour of the block $\boldsymbol{P}$ of the LTIFD system in Fig. 1.

In the SMI context of this series of papers, the input–output behaviour is determined by a state-space model. The key part (of Part 3) in approximating this model is the estimation of the column space of the extended observability matrix from Hankel matrices constructed from the input and perturbed output data.

Since the deterministic part $\boldsymbol{P}$ of the unknown system in Fig. 1 is LTIFD, the above problem statement is equivalent to the basic identification problem stated in Part 2 (Verhaegen and Dewilde 1992 b); however, now $v(k)$ is a zero-mean stochastic process of *arbitrary colouring*. The latter represents the sum of all the time sequences owing to $w_1(k)$, $w_2(k)$ and $v_z(k)$ in Fig. 1 and possibly also due to unmeasurable input sequences. Owing to the output–error approach, but also because the individual effect of the different error sources is difficult to trace back in the recorded output $\tilde{z}(k)$, we treat the latter equivalent problem in this paper.

Instrumental variables are common practice in parametric model identification schemes (see e.g. Söderström and Stoica 1989 and Ljung 1987). The primary purpose in selecting these variables is to remove asymptotically the bias on the estimates due to the perturbation $v(k)$. This can be done in various ways, generally by projection or filtering the input–output data. The second constraint on these instrumental variables or on the projection operation is that the key model information has to be preserved. This is generally stated as a rank constraint. These two constraints also characterize the developed extension of the ordinary MOESP scheme to handle perturbations $v(k)$ of arbitrary colouring. First, the operation of the instrumental variables is presented as a projection of the structured matrices into a subspace constructed from an instrumental variable time sequence. Second, certain matrices affected by the

instrumental variables have to satisfy a rank constraint. Although, different choices of instrumental variables can easily be suggested, they may differ significantly in the way they change the numerical conditioning of the estimation problem at hand. Therefore, we pay special attention to the way the different extensions affect the numerical sensitivity of the key subspace approximation problem. (The organization of this paper is again a continuation of that established in Parts 1 and 2. For a quick review of the relevant notation, model and data representation, we refer to § 2 of Part 1—Verhaegen and Dewilde 1992 a.)

In § 2, we briefly summarize the key algorithmic steps that characterize the ordinary MOESP scheme. The asymptotic unbiasedness of the ordinary MOESP scheme for the equivalent problem stated above is investigated in § 3. Two different types of instrumental variables which can be efficiently included in the algorithmic structure of the (ordinary) MOESP schemes are presented in § 4. The sensitivity study on the effect of error-affected data on the calculation of the column space of the extended observability matrix is made in § 5. The insights obtained in this section are verified by means of two simulation studies based on mathematical models of realistic physical systems; namely a flexible mechanical system and the identification of longitudinal aircraft dynamics using data recorded when flying through a gusty wind field; § 7 concludes this series of papers, summing up some of the useful properties of the approach presented.

2. The relevant algorithmic steps of the ordinary MOESP scheme

The operation of the ordinary MOESP scheme, derived by Verhaegen and Dewilde (1992 a) in Part 1 of this series for the case $v(k) \equiv 0$ is characterized by three key steps.

Step 1. The first key step is the following RQ factorization:

$$\begin{bmatrix} U_{1,i,N} \\ \hline Y_{1,i,N} \end{bmatrix} = \left[\begin{array}{c|c} R_{11} & 0 \\ \hline R_{21} & R_{22} \end{array}\right] \begin{bmatrix} Q_1 \\ \hline Q_2 \end{bmatrix}$$

Step 2. The second key step is the calculation of the column space of the extended observability matrix Γ_i by means of the following SVD:

$$R_{22} = [U_n | U_n^{\perp}] \left[\begin{array}{c|c} S_n & 0 \\ \hline 0 & S_2 \end{array}\right] \begin{bmatrix} V_n^{\mathrm{T}} \\ \hline (V_n^{\perp})^{\mathrm{T}} \end{bmatrix}$$

Let $T \in R^{n \times n}$ be a non-singular matrix, then, as proved in Theorem 4 of Part 1 (Verhaegen and Dewilde 1992 a),

$$\Gamma_i = U_n T^{-1}$$

From the matrix U_n we can compute the pair of matrices (A_T, C_T).

Step 3. The third key step is to use the knowledge of U_n, to transform the data equation

$$Y_{1,i,N} = \Gamma_i X_{1,N} + H_i U_{1,i,N} = R_{21} Q_1 + R_{22} Q_2 \tag{1}$$

into

$$(U_n^{\perp})^{\mathrm{T}} H_i - (U_n^{\perp})^{\mathrm{T}} R_{21} R_{11}^{-1} = 0 \tag{2}$$

From this equation, we can determine the pair of matrices (B_T, D).

3. Asymptotic analysis of the ordinary MOESP scheme

In this section we analyse the unbiasedness of the ordinary MOESP scheme for the equivalent of the realistic open-loop identification problem, stated in the introduction of this paper.

In the first part of this analysis we treat the (asymptotic) effect of the error $v(k)$ on the calculation of the column space of Γ_i. The result of this analysis is summarized in the following theorem.

Theorem 1: *Let*

(1) *the input u_k be such that condition (28) of Part 1 be satisfied;*

(2) *the dimension parameter i in the ordinary MOESP scheme satisfies*

$$i > n \tag{3}$$

(3) *the following RQ factorizations of*

$$\left[\begin{array}{c} U_{1,i,N} \\ \hline Z_{1,i,N} \end{array}\right] \quad \textit{and} \quad \left[\begin{array}{c} U_{1,i,N} \\ \hline X_{1,N} \end{array}\right]$$

be given as

$$\left[\begin{array}{c} U_{1,i,N} \\ \hline Z_{1,i,N} \end{array}\right] = \begin{matrix} mi \\ li \end{matrix} \overbrace{\left[\begin{array}{c|c} R_{11}^N & 0 \\ \hline R_{21}^N & R_{22}^N \end{array}\right]}^{mi \quad li} \left[\begin{array}{c} Q_1^N \\ \hline Q_2^N \end{array}\right] \tag{4}$$

$$\left[\begin{array}{c} U_{1,i,N} \\ \hline X_{1,N} \end{array}\right] = \begin{matrix} mi \\ n \end{matrix} \overbrace{\left[\begin{array}{c|c} R_{11}^N & 0 \\ \hline R_{x1}^N & R_{x2}^N \end{array}\right]}^{mi \quad n} \left[\begin{array}{c} Q_1^N \\ \hline Q_x^N \end{array}\right] \tag{5}$$

(4) *the following limits hold:*

$$\lim_{N\to\infty} \frac{1}{N} U_{1,i,N} U_{1,i,N}^{\mathrm{T}} = R_u \tag{6}$$

$$\lim_{N\to\infty} \frac{1}{N} V_{1,i,N} V_{1,i,N}^{\mathrm{T}} = R_v \tag{7}$$

$$\lim_{N\to\infty} \frac{1}{N} R_{x1}^N (R_{x1}^N)^{\mathrm{T}} + \lim_{N\to\infty} \frac{1}{N} R_{x2}^N (R_{x2}^N)^{\mathrm{T}} = P_{x1} + P_{x2} \tag{8}$$

$$\lim_{N\to\infty} \frac{1}{N} U_{1,i,N} V_{1,i,N}^{\mathrm{T}} = 0 \tag{9}$$

$$\lim_{N\to\infty} \frac{1}{N} X_{1,N} V_{1,i,N}^{\mathrm{T}} = 0 \tag{10}$$

then

$$\lim_{N\to\infty} \frac{1}{N} R_{22}^N (R_{22}^N)^T = \Gamma_i P_{x2} \Gamma_i^T + R_v \tag{11}$$

For the proof, see Appendix A.

If we substitute the matrix product $\Gamma_i P_{x2} \Gamma_i^T$ by its SVD $U_\Gamma S_\Gamma U_\Gamma^T$, with $S_\Gamma \in R^{n\times n}$, then (11) becomes

$$\lim_{N\to\infty} \frac{1}{N} R_{22}^N (R_{22}^N)^T = U_\Gamma S_\Gamma U_\Gamma^T + R_v \tag{12}$$

Hence, according to Proposition 2 of Appendix B of Part 2 (Verhaegen and Dewilde 1992 b), the ordinary MOESP scheme will determine the column space of the extended observability matrix Γ_i asymptotically unbiasedly, only when the (covariance) matrix R_v is proportional to the identity matrix. This constraint on the matrix R_v corresponds to v_k being zero-mean white noise.

In the second part, we analyse the effect of the errors v_k on the calculations of the matrices $[B_T, D]$ from (2). Let the column space of Γ_i be denoted by U_n and its orthogonal complement by $U_n^\perp$, then (1), for $v(k) \neq 0$, becomes

$$U_n T^{-1} X_{1,N} + H_i U_{1,i,N} + V_{1,i,N} = R_{21}^N Q_1^N + R_{22}^N Q_2^N$$

Since $(U_n^\perp)^T U_n = 0$, multiplication of this equation on the left by $(U_n^\perp)^T$ yields

$$(U_n^\perp)^T H_i U_{1,i,N} + (U_n^\perp)^T V_{1,i,N} = (U_n^\perp)^T R_{21}^N Q_1^N + (U_n^\perp)^T R_{22}^N Q_2^N$$

When the condition (28) of Part 1 is fulfilled $\rho(U_{1,i,N}) = mi$, we can multiply the above equation on the left by the right inverse of $U_{1,i,N}$ and obtain

$$(U_n^\perp)^T H_i + (U_n^\perp)^T V_{1,i,N} (Q_1^N)^T (R_{11}^N)^{-1} = (U_n^\perp)^T R_{21}^N (R_{11}^N)^{-1}$$

Using, the expression for $V_{1,i,N}(Q_1^N)^T$ in (58) of the proof of Theorem 1, yields

$$(U_n^\perp)^T H_i + (U_n^\perp)^T \varepsilon_N^6 E_N^6 \left(\frac{1}{N} R_{11}^N (R_{11}^N)^T \right)^{-1} = (U_n^\perp)^T R_{21}^N (R_{11}^N)^{-1}$$

Hence, in the limit,

$$\lim_{N\to\infty} (U_n^\perp)^T R_{21}^N (R_{11}^N)^{-1} = (U_n^\perp)^T H_i \tag{13}$$

Therefore, we conclude that when the column space of Γ_i is known, the matrix pair $[B_T, D]$ can be computed asymptotically unbiased. The latter conclusion holds for the case where the error term v_k is zero-mean arbitrarily coloured noise independent of u_k. Hence, this outline stresses the key role played by the computation of the subspace determined by the column space of the extended observability matrix Γ_i.

Remark 1: The restriction imposed on the colouring of the perturbation v_k when the column space of Γ_i has to be computed asymptotically unbiased can be removed when the covariance matrix R_v of this error source is known. The computation of the column space of Γ_i then proceeds via a generalized SVD (Paige and Saunders 1981) instead of an ordinary SVD. The modification of the algorithm in this case is similar to that required when making the scheme described by Moonen *et al.* (1989) applicable to zero-mean errors of known

colouring. Therefore, we refer to Moonen and Vandewalle (1990) for algorithmic details. In a practical context, the colouring of the different noise processes in Fig. 1 is generally not known. □

4. Incorporating instrumental variables in the ordinary MOESP scheme

In the previous section it was demonstrated that the ordinary MOESP scheme is only capable of solving the basic identification problem, defined in Part 2, asymptotically unbiased. It would be possible to extend the applicability of this scheme to a broader class of perturbations via the introduction of the so-called instrumental variables.

In the class of parametric model identification schemes (see Söderström and Stoica 1989 or Ljung 1987) the use of instrumental variables is common practice. In this paper, we demonstrate how some of these ideas carry over to the ordinary MOESP scheme.

4.1. *General operation of instrumental variables in the ordinary MOESP scheme*

Assume that the signal referred to as the instrumental variable gives rise to the *instrumental variable matrix* $W_N \in R^{j\times N}$ (for $j \geqslant n$). Recall (59) from the proof of Theorem 1, namely

$$\frac{1}{\sqrt{N}} R_{22}^N Q_2^N = -\varepsilon_N^6 E_N^6 \left(\frac{1}{\sqrt{N}} (R_{11}^N)^T\right)^{-1} Q_1^N + \frac{1}{\sqrt{N}} \Gamma_i R_{x2}^N Q_x^N + \frac{1}{\sqrt{N}} V_{1,i,N} \tag{14}$$

Then the use of instrumental variables in the ordinary MOESP schemes corresponds to the multiplication on the right of (14) by the matrix W_N^T, i.e.

$$\frac{1}{\sqrt{N}} R_{22}^N Q_2^N W_N^T = \frac{1}{\sqrt{N}} \Gamma_i R_{x2}^N Q_x^N W_N^T - \varepsilon_N^6 E_N^6 \left(\frac{1}{\sqrt{N}} (R_{11}^N)^T\right)^{-1} Q_1^N W_N^T + \frac{1}{\sqrt{N}} V_{1,i,N} W_N^T \tag{15}$$

Assuming that

$$\lim_{N\to\infty} \left(\frac{1}{\sqrt{N}} (R_{11}^N)^T\right)^{-1} Q_1^N W_N^T$$

exists, then (15) in the limit $N \to \infty$ becomes

$$\lim_{N\to\infty} \frac{1}{\sqrt{N}} R_{22}^N Q_2^N W_N^T = \lim_{N\to\infty} \frac{1}{\sqrt{N}} \Gamma_i R_{x2}^N Q_x^N W_N^T + \lim_{N\to\infty} \frac{1}{\sqrt{N}} V_{1,i,N} W_N^T \tag{16}$$

From this equation we conclude that, when the instrumental variables are chosen such that: (1) they are statistically independent from the error term v_k, i.e.

$$\lim_{N\to\infty} \frac{1}{\sqrt{N}} V_{1,i,N} W_N^T = 0$$

and (2)

$$\rho\left(\lim_{N\to\infty}\frac{1}{\sqrt{N}}\,\Gamma_i R_{x2}^N Q_x^N W_N^{\mathrm{T}}\right) = n$$

the column space of Γ_i is computed asymptotically unbiasedly for arbitrary zero-mean errors v_k independent of the input u_k. A similar pair of conditions is imposed in the parameter model identification framework (see e.g. Ljung 1987, p. 193). Two types of extensions of the ordinary MOESP scheme based on instrumental variables are discussed in more detail. First, in § 4.2 we describe the extension based on past input measurements and, second, in § 4.3 we describe the extension based on reconstructed state quantities. In § 5 we investigate the numerical sensitivity introduced by these extensions on the computation of the column space of the matrix Γ_i.

4.2. *Past observations of the input sequence as instrumental variables*

In this subsection, we assume the following data samples of the input $u(k)$ and the output $\tilde{z}(k)$ to be available:

$$u(1),\ u(2),\ \ldots,\ u(i),\ u(i+1),\ \ldots,\ u(N+2i-1) \tag{17}$$

$$\tilde{z}(1),\ \tilde{z}(2),\ \ldots,\ \tilde{z}(i),\ \tilde{z}(i+1),\ \ldots,\ \tilde{z}(N+2i-1) \tag{18}$$

With these observations, the instrumental variable matrix W_N is taken equal to $U_{1,i,N}/\sqrt{N}$. From (16) we might conclude that the use of the instrumental variable matrix requires the accumulation of the orthogonal transformation Q_2^N. Based on the present choice of instrumental variables, a more efficient implementation is possible.

The PI (ordinary MOESP with instrumental variables constructed from the Past Input sequence) algorithm (Error-free case). Given:

The input to the ordinary MOESP scheme (see § 5.2 of Part 1—Verhaegen and Dewilde 1992 a), with the input and output data sequences given in (17) and (18) for $v(k) \equiv 0$.

Algorithmic steps:

Step 1. Construct the Hankel matrices $U_{1,i,N}$, $U_{i+1,i,N}$ and $Y_{i+1,i,N}$.

Step 2. Compute the following RQ factorization, without accumulating the orthogonal transformations required:

$$\left[\begin{array}{c} U_{i+1,i,N} \\ \hline Y_{i+1,i,N} \\ \hline U_{1,i,N} \end{array}\right] = \begin{array}{c} \\ mi \\ li \\ mi \end{array}\overset{\begin{array}{ccc} mi & li & mi \end{array}}{\left[\begin{array}{c|c|c} R_{11} & 0 & 0 \\ \hline R_{21} & R_{22} & 0 \\ \hline R_{31} & R_{32} & R_{32} \end{array}\right]}\left[\begin{array}{c} Q_1 \\ \hline Q_2 \\ \hline Q_3 \end{array}\right] \tag{19}$$

Step 3. Compute the SVD of the matrix $R_{22}R_{32}^{\mathrm{T}}$, denoted as

$$R_{22}R_{32}^{\mathrm{T}} = \overset{n}{li}[\overset{n}{U_n}|\overset{li-n}{U_n^{\perp}}]\left[\begin{array}{c|c} \overset{n}{S_n} & \overset{mi-n}{0} \\ \hline 0 & S_2 \end{array}\right] V^{\mathrm{T}} \tag{20}$$

Step 4. Calculation of the quadruple $[A_{\mathrm{T}}, B_{\mathrm{T}}, C_{\mathrm{T}}, D]$, as outlined in Step 4 of the ordinary MOESP scheme in § 5.2 of Part 1 (Verhaegen and Dewilde 1992 a).

Based on the assumption that the error $v(k)$ and the input $u(k)$ are independent, condition (1) imposed on the instrumental variables holds.

In the error-free case, the matrix product $R_{22}R_{32}^{\mathrm{T}}$ equals

$$R_{22}R_{32}^{\mathrm{T}} = \Gamma_i R_{x2} Q_x U_{1,i,N}^{\mathrm{T}} \tag{21}$$

Therefore, when $\rho(R_{22}R_{32}^{\mathrm{T}}) = n$, the SVD in (20) allows for the computation of the column space of Γ_i. The fulfillment of this condition, corresponding to condition (2) imposed on the instrumental variables, depends on the actual input used. For example, when a periodic input signal of the particular class treated in § 3.3 of Part 1 (Verhaegen and Dewilde 1992 a) is used, exactly the same conditions as stipulated in Theorem 2 of Part 1 are required. This can be proved in a similar way as done in the proof of Theorem 2 of Part 1. When the input is a zero-mean white noise sequence, this condition is also satisfied and we refer to § 5.3 for more details.

4.3. *Reconstructed state variables as instrumental variables*

4.3.1. *Reconstructing the state variables.* In the MOESP framework, a second possible choice of instrumental variables is based on the approximation of the space spanned by the rows of the matrix $X_{1,N}$. The state quantities that give rise to this space are assumed not to be known exactly. Therefore, they have to be reconstructed from the available input–output observations (and a possible state-space model estimate). In this paper, we only outline a simple way of reconstructing the state vector sequence $(TX)_{1,N}$. The reconstruction requires: (1) an estimate of the state space quadruple, denoted as $[\hat{A}_{\mathrm{T}}, \hat{B}_{\mathrm{T}}, \hat{C}_{\mathrm{T}}, \hat{D}]$; and (2) an estimate of the initial state $\eta_1 = Tx_1$. The estimated state vector sequence, denoted by $[\hat{\eta}_1, \hat{\eta}_2, \ldots, \hat{\eta}_N]$, is then calculated from the difference equation

$$\hat{\eta}_{k+1} = \hat{A}_T \hat{\eta}_k + \hat{B}_T u_k \tag{22}$$

Two possibilities are discussed in this paper to obtain an estimated state-space quadruple. First, using the ordinary MOESP scheme and second using the PI scheme. The estimate of η_1 is discussed next. Assume the system matrices $[A_T, B_T, C_T, D]$ to be given then, similarly to (1), we can denote the output sequence $Y_{1,N,1}$ as

$$Y_{1,N,1} = (\Gamma_N T^{-1})\eta_1 + \underbrace{H_N U_{1,N,1}}$$

where the underbraced term is the simulated output of the system determined by the quadruple $[A_T, B_T, C_T, D]$ with input sequence $U_{1,N,1}$ and zero initial conditions. When the system $[A_T, B_T, C_T, D]$ is observable, the initial state vector η_1 equals

$$\eta_1 = (\Gamma_N T^{-1})\dagger(Y_{1,N,1} - H_N U_{1,N,1})$$

where $(\cdot)\dagger$ denotes the pseudo-inverse of the matrix $(\cdot)$. When we make use of the actual output measurements $\{\tilde{z}(k)\}$, the following estimate:

$$\hat{\eta}_1 = (\Gamma_N T^{-1})\dagger(\tilde{Z}_{1,N,1} - H_N U_{1,N,1})$$

is asymptotically unbiased. This is because the errors $v(k)$ are independent from the deterministic sequences determined by the columns of the matrix $(\Gamma_n T^{-1})$. Finally, using a model estimate $[\hat{A}_T, \hat{B}_T, \hat{C}_T, \hat{D}]$, we define the following estimate:

$$\hat{\eta}_1 = (\widehat{\Gamma_N T^{-1}})\dagger(\tilde{Z}_{1,N,1} - \hat{H}_N U_{1,N,1})$$

Due to the model errors, this latter quantity will generally be biased. As a consequence, the reconstructed state quantities will be erroneous. Nevertheless, the following lemma highlights their usefulness.

Lemma 1: *Let $\eta_k \in R^n$, $u_k \in R^m$ and $\Phi \in R^{n\times n}$ be an asymptotically stable matrix and let $\Gamma \in R^{n\times m}$, $\eta_1 \in R^n$ be an arbitrary, bounded, constant matrix and vector. Let these quantities define a linear time-invariant system as follows:*

$$\eta_{k+1} = \Phi\eta_k + \Gamma u_k$$

Furthermore, let u_k and v_l be two ergodic, independent zero-mean stochastic processes, then

$$\lim_{N\to\infty} \frac{1}{N} \sum_{j=1}^{N} \eta_{j+1} v_{j+l-1}^{\mathrm{T}} = 0 \quad \forall l$$

For the proof, see Appendix B.

Therefore, we conclude that, although the actual estimates of $\hat{A}_T$, $\hat{B}_T$ and $\hat{\eta}_1$ are affected by the noise $v(k)$, the fact that they are constant over the reconstruction interval $k \geqslant 1$ guarantees that the reconstructed state sequence satisfies condition (1) imposed on the instrumental variables.

4.3.2. *A compact implementation.* With the reconstructed state sequence $(\widehat{TX})_{1,N}$, we can state the following algorithm.

The RS (ordinary MOESP with instrumental variables constructed from the Reconstructed State vector sequence) algorithm (Error-free case). Given:

The input to the ordinary MOESP scheme (see § 5.1 of Part 1—Verhaegen and Dewilde 1992 a), and
the state vector sequence $(TX)_{1,N}$.

Algorithmic steps:

Step 1. Compute the SVD of the state vector sequence $(TX)_{1,N}$, denoted as

$$(TX)_{1,N} = U_{(TX)} S_{(TX)} V_{(TX)}^{\mathrm{T}} \tag{23}$$

(In this step we could restrict to the computationally more efficient RQ factorization of $(TX)_{1,N}$.)

Step 2. Construct the Hankel matrices $U_{1,i,N}$ and $Y_{1,i,N}$.

Step 3. Compute the following RQ factorization, without accumulating the orthogonal transformations required:

$$\begin{bmatrix} U_{1,i,N} \\ \hline Y_{1,i,N} \\ \hline V_{(TX)}^{\mathrm{T}} \end{bmatrix} = \begin{matrix} mi \\ li \\ mi \end{matrix} \overset{\begin{matrix} mi & li & n \end{matrix}}{\left[\begin{array}{c|c|c} R_{11} & 0 & 0 \\ \hline R_{21} & R_{22} & 0 \\ \hline R_{31} & R_{32} & R_{32} \end{array}\right]} \begin{bmatrix} Q_1 \\ \hline Q_2 \\ \hline Q_3 \end{bmatrix} \tag{24}$$

Step 4. Compute the SVD of the matrix $R_{22}R_{32}^{\mathrm{T}}$, denoted as

$$R_{22}R_{32}^{\mathrm{T}} = \overset{\begin{matrix} n & li-n \end{matrix}}{li\left[U_n \middle| U_n^{\perp}\right]} \begin{bmatrix} S_n \\ \hline 0 \end{bmatrix}^{n} V^{\mathrm{T}} \tag{25}$$

Step 5. Equivalent to Step 4 of the ordinary MOESP scheme in § 5.2 of Part 1 (Verhaegen and Dewilde 1992 a).

In the error-free case, the matrix product $R_{22}R_{32}^{\mathrm{T}}$ now equals

$$R_{22}R_{32}^{\mathrm{T}} = \Gamma_i R_{x2} Q_x V_{(TX)} \tag{26}$$

From (5) and (23), we have the following relationship:

$$U_{(TX)}S_{(TX)}V_{(TX)}^{\mathrm{T}} = TR_{x1}Q_1 + TR_{x2}Q_x$$

Multiplying both sides on the right by Q_x^{T} and making use of the fact that $Q_1Q_x^{\mathrm{T}} = 0$, $Q_xQ_x^{\mathrm{T}} = I$ yields

$$U_{(TX)}S_{(TX)}V_{(TX)}^{\mathrm{T}}Q_x^{\mathrm{T}} = TR_{x2}$$

Hence, when condition (28) of Part 1 (Verhaegen and Dewilde 1992 a) is fulfilled, Lemma 1 of Part 1 shows that the rank of the matrix product $Q_xV_{(TX)}$ is n. Therefore, when using the row space of the error-free state vector sequence $X_{1,N}$ as instrumental variables, Condition (2) imposed on these quantities in § 4.1 will also be satisfied.

5. Comparison of the two instrumental variable ordinary MOESP schemes

5.1. *Framework of analysis*

In this section, we compare the two extensions of the ordinary MOESP scheme. The comparison study investigates the sensitivity of the calculated quantities with respect to the perturbation $v(k)$. More precisely, since the extended observability matrix Γ_i has been demonstrated to be a key quantity in the operation of the (ordinary) MOESP scheme, see for example the asymptotic analysis study in § 3, the column space of the latter matrix is taken as the quantity of interest and the perturbation considered is the term

$$\frac{1}{\sqrt{N}} V_{1,i,N}W_N^{\mathrm{T}} - \varepsilon_N^6 E_N^6 \left(\frac{1}{\sqrt{N}} (R_{11}^N)^{\mathrm{T}}\right)^{-1} Q_1^N W_N^{\mathrm{T}}$$

in (15). This perturbation approaches zero for $N \to \infty$, however for finite N, it causes an error in the approximation of the column space of Γ_i. Therefore, we

study the effect of the above perturbation on the calculated column space of the matrix $R_{22}^N Q_2^N W_N^T/\sqrt{N}$ via a SVD.

Assuming, as in § 3.2 of Part 2, that the effect of the perturbations is of different orders of magnitude larger than the errors made during the numerical computations, we investigate the influence of the perturbations on the calculation of the invariant subspaces in a symmetric eigenvalue problem. Hence, in this sensitivity analysis we shall again make use of Proposition 1 of Appendix B of Part 2 (Verhaegen and Dewilde 1992 b).

The actual experimental conditions for which the comparative sensitivity study is performed correspond to the case where the input signal is a zero-mean white noise sequence with variance σ_u^2. Further, we shall assume, in § 5.3, that the subspace spanned by the state vector sequence in the matrix $X_{1,N}$ is exactly known. In the discussion in § 5.4, the effect of using reconstructed state quantities is discussed in more detail.

5.2. *The perturbed SVD problem with the PI scheme*

Equation (14) for the matrices appearing in the PI scheme reads

$$\frac{1}{\sqrt{N}} R_{22}^N Q_2^N = -\varepsilon_N^6 E_N^6 \left(\frac{1}{\sqrt{N}} (R_{11}^N)^T\right)^{-1} Q_1^N + \frac{1}{\sqrt{N}} \Gamma_i R_{x2}^N Q_x^N + \frac{1}{\sqrt{N}} V_{i+1,i,N} \tag{27}$$

With some abuse of notation, we recall (33) of Part 1 from the noise-free case (Verhaegen and Dewilde 1992 a)

$$\Gamma_i R_{x2} Q_x = R_{22} Q_2$$

Furthermore, in the same noise-free case, the proof of Theorem 1 of Part 1 shows that due to the white noise property of the input $u(k)$, see the equation just before (A 6) of Part 1, the matrix product $R_{22}^N Q_2^N/\sqrt{N}$ equals

$$\frac{1}{\sqrt{N}} R_{22}^N Q_2^N = \Gamma_i \left[\frac{1}{\sqrt{N}} X_{1,N} - \varepsilon_N^3 E_N^3 \left(\frac{1}{\sqrt{N}} (R_{11}^N)^T\right)^{-1} Q_1^N\right]$$

Combining the last two equations and again adapting their indices to those of the matrices used in the PI scheme, shows that the error-free term $\Gamma_i R_{x2}^N Q_x^N/\sqrt{N}$ in (27), equals

$$\Gamma_i \left(\frac{1}{\sqrt{N}} X_{i+1,N} - \varepsilon_N^3 E_N^3 \left(\frac{1}{\sqrt{N}} (R_{11}^N)^T\right)^{-1} Q_1^N\right)$$

and hence, (27) becomes

$$\frac{1}{\sqrt{N}} R_{22}^N Q_2^N = \Gamma_i \frac{1}{\sqrt{N}} X_{i+1,N} - \underbrace{(\Gamma_i \varepsilon_N^3 E_N^3 + \varepsilon_N^6 E_N^6)}_{=: \varepsilon_N^9 E_N^9} \left(\frac{1}{\sqrt{N}} (R_{11}^N)^T\right)^{-1} Q_1^N + \frac{1}{\sqrt{N}} V_{i+1,i,N} \tag{28}$$

Using this expression for $R_{22}^N Q_2^N/\sqrt{N}$, the matrix product $R_{22} R_{32}^T$ in (21) scaled by a factor $1/N$ equals

$$\frac{1}{N} R_{22}^N Q_2^N U_{1,i,N}^T = \Gamma_i \underbrace{\frac{1}{N} X_{i+1,N} U_{1,i,N}^T}_{\text{(i)}} - \varepsilon_N^9 E_N^9 \left(\frac{1}{\sqrt{N}} (R_{11}^N)^T \right)^{-1} \underbrace{\frac{1}{\sqrt{N}} Q_1^N U_{1,i,N}^T}_{\text{(ii)}}$$

$$+ \underbrace{\frac{1}{N} V_{i+1,i,N} U_{1,i,N}^T}_{\text{(iii)}} \tag{29}$$

We now explicitly evaluate the underbraced terms.

(i) Using the convolution expression for $X_{i+1,N}$ as in (A7) of Part 1 (Verhaegen and Dewilde 1992 a) for $X_{1,N}$ we obtain

$$\frac{1}{N} X_{i+1,N} U_{1,i,N}^T =$$

$$\frac{1}{N} [B \quad AB \quad \dots \quad A^{i-1}B | A^iB \quad \dots] \left[\begin{array}{cccc} u_i & u_{i+1} & \dots & u_{N+i-1} \\ u_{i-1} & u_i & \dots & \\ \vdots & & & \vdots \\ u_1 & u_2 & \dots & u_N \\ \hline u_0 & & \dots & u_{N-1} \\ u_{-1} & & & \\ \vdots & & & \vdots \end{array} \right] U_{1,i,N}^T$$

Using the white noise property of the input $u(k)$, the right-hand side of this equation reduces to

$$= [A^{i-1}B \quad \dots \quad AB \quad B | A^iB \quad \dots \quad] \left[\begin{array}{c} \sigma_u^2 I_{m.i} + \varepsilon_N^{10} E_N^{10} \\ \hline \varepsilon_N^{11} E_N^{11} \end{array} \right]$$

(ii) Again using the white noise property of the input $u(k)$, we have

$$\frac{1}{N} U_{i+1,i,N} U_{1,i,N}^T = \varepsilon_N^{12} E_N^{12}$$

Substituting the expression for $U_{i+1,i,N} = R_{11}^N Q_1^N$ in (19) into the above equation yields

$$\frac{1}{\sqrt{N}} Q_1^N U_{1,i,N}^T = \left(\frac{1}{\sqrt{N}} R_{11}^N \right)^{-1} \varepsilon_N^{12} E_N^{12}$$

(iii) Finally, using the independency of the perturbation $v(k)$ and the input $u(k)$ we obtain

$$\frac{1}{N} V_{i+1,i,N} U_{1,i,N}^T = \varepsilon_N^{13} E_n^{13}$$

Substituting the results of the above three different items back into (29) yields

$$\frac{1}{N} R_{22}^N Q_2^N U_{1,i,N}^T = \Gamma_i [A^{i-1}B \quad \dots \quad AB \quad B | A^iB \quad \dots] \left[\begin{array}{c} \sigma_u^2 I_{m.i} + \varepsilon_N^{10} E_N^{10} \\ \hline \varepsilon_N^{11} E_N^{11} \end{array} \right]$$

$$- \varepsilon_N^9 E_N^9 \left(\frac{1}{N} R_{11}^N (R_{11}^N)^T \right)^{-1} \varepsilon_N^{12} E_N^{12} + \varepsilon_N^{13} E_N^{13} \tag{30}$$

5.3. *The perturbed SVD problem with the RS scheme*

Similarly to (28) in the previous section, the matrix $R_{22}^N Q_2^N/\sqrt{N}$ occurring in the RS scheme can be expressed as

$$\frac{1}{\sqrt{N}} R_{22}^N Q_2^N = \Gamma_i \frac{1}{\sqrt{N}} X_{1,N} - \varepsilon_N^9 E_N^9 \left(\frac{1}{\sqrt{N}} (R_{11}^N)^T\right)^{-1} Q_1^N + \frac{1}{\sqrt{N}} V_{1,i,N}$$

Let us assume that the row space of the matrix $(TX)_{1,N}$ is known. Hence, the matrix product $R_{22}R_{32}^T$ in (26) scaled by a factor $1/\sqrt{N}$ equals

$$\frac{1}{\sqrt{N}} R_{22}^N Q_2^N V_{(TX)}^N = \Gamma_i \underbrace{\frac{1}{\sqrt{N}} X_{1,N} V_{(TX)}^N}_{\text{(i)}} - \varepsilon_N^9 E_N^9 \left(\frac{1}{\sqrt{N}} (R_{11}^N)^T\right)^{-1} \underbrace{Q_1^N V_{(TX)}^N}_{\text{(ii)}}$$

$$+ \underbrace{\frac{1}{\sqrt{N}} V_{1,i,N} V_{(TX)}^N}_{\text{(iii)}} \tag{31}$$

Again we explicitly evaluate the underbraced terms.

(i) With the SVD of $X_{1,N}$ given as

$$X_{1,N} = U_X^N S_X^N (V_X^N)^T \tag{32}$$

the first underbraced term becomes

$$\frac{1}{\sqrt{N}} X_{1,N} V_{(TX)}^N = U_X^N \frac{S_X^N}{\sqrt{N}} (V_X^N)^T V_{(TX)}^N$$

Since the row spaces of the matrices $X_{1,N}$ and $(TX)_{1,N}$ are equal, the matrix $[(V_X^N)^T V_{(TX)}^N]$ satisfies

$$[(V_X^N)^T V_{(TX)}^N][(V_X^N)^T V_{(TX)}^N]^T = I \tag{33}$$

(ii) Since the input $u(k)$ is white noise, we have, by Lemma 2 of Part 1 (Verhaegen and Dewilde 1992 a),

$$\frac{1}{N} U_{1,i,N} X_{1,N}^T T^T = \varepsilon_N^3 E_N^3$$

Substituting the expression for $U_{1,i,N} = R_{11}^N Q_1^N$ given in (24) and that for $(TX)_{1,N}$ given in (23), into the above equation yields

$$Q_1^N V_{(TX)}^N = \left(\frac{1}{\sqrt{N}} R_{11}^N\right)^{-1} \varepsilon_N^3 E_N^3 (U_{(TX)}^N)^T \left(\frac{1}{\sqrt{N}} S_{(TX)}^N\right)^{-1}$$

(iii) Finally, according to Lemma 1, we obtain

$$\frac{1}{\sqrt{N}} V_{1,i,N} V_{(TX)}^N = \varepsilon_N^{14} E_N^{14} (U_{(TX)}^N)^T \left(\frac{1}{\sqrt{N}} S_{(TX)}^N\right)^{-1}$$

Substituting the results of the above three different items back into (31) yields

$$\frac{1}{N} R_{22}^N Q_2^N V_{(TX)}^N = \Gamma_i U_X^N \frac{S_X^N}{\sqrt{N}} [(V_X^N)^T V_{(TX)}^N] - \left[\varepsilon_N^9 E_N^9 \left(\frac{1}{N} R_{11}^N (R_{11}^N)^T\right)^{-1} \varepsilon_N^3 E_N^3 + \varepsilon_N^{14} E_N^{14}\right] (U_{(TX)}^N)^T \left(\frac{S_{(TX)}^N}{\sqrt{N}}\right)^{-1} \quad (34)$$

5.4. *Discussion*

To apply Proposition 1 of Part 2 (Verhaegen and Dewilde 1991 b) we multiply both sides of (30) by their transposes. Denoting the matrix $[B \; AB \; \ldots \; A^{i-1}B]$ and $[A^iB \; \ldots \;]$ respectively by Δ_i and Δ_r, we obtain for the PI scheme

$$\frac{1}{N^2} R_{22}^N Q_2^N U_{1,i,N}^T U_{1,i,N} (Q_2^N)^T (R_{22}^N)^T = \sigma_u^4 \Gamma_i \Delta_i \Delta_i^T \Gamma_i^T + \Delta_{PI} \quad (35)$$

where Δ_{PI} represents second-order effects that vanish for $N \to \infty$.

To find a similar expression for the RS scheme, we first use the expression for $X_{1,N}$ in (A 7) of Part 1 (Verhaegen and Dewilde 1992 a) and the white noise property of $u(k)$ to derive the following equality:

$$\lim_{N\to\infty} \frac{1}{N} X_{1,N} X_{1,N}^T = \lim_{N\to\infty} \frac{1}{N} U_X^N S_X^2 (U_X^N)^T = \sigma_u^2 [\Delta_i | \Delta^r] \begin{bmatrix} \Delta_i^T \\ (\Delta^r)^T \end{bmatrix}$$

Hence, multiplication of both sides of (34) by their transposes, and making use of the relationship in (33) yields

$$\frac{1}{N} R_{22}^N Q_2^N V_X^N (V_X^N)^T (Q_2^N)^T (R_{22}^N)^T = \sigma_u^2 \Gamma_i [\Delta_i | \Delta^r] \begin{bmatrix} \Delta_i^T \\ (\Delta^r)^T \end{bmatrix} \Gamma_i^T + \Delta_{RS} \quad (36)$$

where again Δ_{RS} represents second-order effects that vanish for $N \to \infty$.

Based on similar reasoning as performed in the sensitivity analysis in § 3.2.3 of Part 2 (Verhaegen and Dewilde 1992 b), an application of Proposition 1 of Part 2 leads to the following observation. When the perturbations Δ_{PI} in (35) and Δ_{RS} in (36) are comparable, the calculation of the column space of Γ_i with the PI scheme is much more sensitive to the perturbations on the data than is the case with the RS scheme, when the following condition holds:

$$\Gamma_i [\Delta_i | \Delta^r] \begin{bmatrix} \Delta_i^T \\ (\Delta^r)^T \end{bmatrix} \Gamma_i^T \gg \Gamma_i \Delta_i \Delta_i^T \Gamma_i^T \quad (37)$$

This increased robustness of the RS scheme depends on the exact knowledge of the state vector sequence in the matrix $X_{1,N}$. In practice we cannot make this assumption. Therefore, we continue the discussion by investigating the effect of only having an approximation of the state vector sequence. Suppose we have an estimate available of the state-space model of the deterministic plant $\boldsymbol{P}$, then we can compute the state vector sequence of this model using the input sequence $u(k)$, as done in § 4.3.1. If we denote the latter state vector sequence by $\hat{X}_{1,N}$, then the SVD in (23) changes into

$$\hat{X}_{1,N} = \hat{U}_X^N \hat{S}_X^N (\hat{V}_X^N)^T \quad (38)$$

and, as a consequence, we use the matrix $\hat{V}_X^N$ in (31) instead of the matrix $V_{(TX)}^N$. In that case, the first two underbraced terms in (31) change into:

(i) With the SVD of $X_{1,N}$ in (32) and of $\hat{X}_{1,N}$ in (38), the first underbraced term becomes

$$\frac{1}{\sqrt{N}} X_{1,N}\hat{V}_X^N = U_X^N S_X^N((V_X^N)^T\hat{V}_X^N)$$

(ii) Since the estimated state vector sequence $\hat{X}_{1,N}$ is also derived from the white noise input $u(k)$, we have, according to Lemma 2 of Part 1 (Verhaegen and Dewilde 1992 a),

$$\frac{1}{N} U_{1,i,N}\hat{X}_{1,N}^T = \varepsilon_N^3 E_N^3$$

and, therefore, by arguments similar to those used in (ii) above:

$$Q_1^N\hat{V}_X^N = \left(\frac{1}{\sqrt{N}} R_{11}^N\right)^{-1}\varepsilon_N^3 E_N^3(\hat{U}_X^N)^T\left(\frac{1}{\sqrt{N}} \hat{S}_X^N\right)^{-1}$$

Again, according to Lemma 1, the last underbraced term remains similar to that in item (iii) of § 5.3. As a consequence, (34) modifies due to the use of reconstructed state quantities into

$$\frac{1}{\sqrt{N}} R_{22}^N Q_2^N\hat{V}_X^N = \Gamma_i U_X^N \frac{S_X^N}{\sqrt{N}}((V_X^N)^T\hat{V}_X^N) - \left[\varepsilon_N^9 E_N^9\left(\frac{1}{N} R_{11}^N(R_{11}^N)^T\right)^{-1}\varepsilon_N^3 E_N^3 + \varepsilon_N^{14} E_N^{14}\right](\hat{U}_X^N)^T\left(\frac{\hat{S}_X^N}{\sqrt{N}}\right)^{-1} \quad (39)$$

Since the row space of the matrices $X_{1,N}$ and $\hat{X}_{1,N}$ do not necessarily coincide, the matrix $((V_X^N)^T\hat{V}_X^N)$ generally is a contraction now, that is $\|(V_X^N)^T\hat{V}_X^N\| \leq 1$, and therefore

$$U_X^N \frac{S_X^N}{\sqrt{N}}(I - ((V_X^N)^T\hat{V}_X^N)((V_X^N)^T\hat{V}_X^N)^T)\frac{S_X^N}{\sqrt{N}}(U_X^N)^T \geq 0 \quad (40)$$

This shows that the smallest singular value of the matrix

$$U_X^N \frac{S_X^N}{\sqrt{N}}((V_X^N)^T\hat{V}_X^N)$$

is less than or equal to that of the matrix

$$U_X^N \frac{S_X^N}{\sqrt{N}}[(V_X^N)^T V_{(TX)}^N]$$

Then, Proposition 1 of Part 2 (Verhaegen and Dewilde 1992 b) shows that when the perturbations which vanish for $N \to \infty$ in (34) and (39) are comparable; the use of imperfect state quantities increases the sensitivity of the calculations in the RS scheme. In particular, the calculations related to the badly reconstructed state quantities will become more sensitive. Let us illustrate this assertion with an example. Suppose the SVD of the matrix $X_{1,N}$ is partitioned as

$$X_{1,N} = [U_1|U_2]\left[\begin{array}{c|c} S_1 & 0 \\ \hline 0 & S_2 \end{array}\right]\left[\begin{array}{c} V_1^T \\ \hline V_2^T \end{array}\right]$$

with $S_1 > S_2$. Similarly, partition the SVD of $\hat{X}_{1,N}$. Furthermore, let a matrix V_3 exist such that $V_3^T V_3 = I$; $V_3^T[V_1|V_2] = 0$ and the following conditions hold:

$$\hat{V}_1 = V_1(I + \Delta_1) + V_2\Delta_2 + V_3\Delta_3$$
$$\hat{V}_2 = V_1\Delta_1' + V_2\Delta_2' + V_3(I + \Delta_3')$$

with $\|\Delta_j\| \approx \|\Delta_j'\| \ll 1$ for $j = 1{:}3$. This assumption, on the row space of $\hat{X}_{1,N}$, reflects the situation that the 'dominant' modes in V_1 are accurately reconstructed whereas the 'weak' modes in V_2 are poorly reconstructed. Then, the term

$$U_X^N \frac{S_X^N}{\sqrt{N}} ((V_X^N)^T \hat{V}_X^N) \quad \text{equals} \quad [U_1|U_2]\left[\left[\begin{array}{c|c} S_1 & 0 \\ \hline 0 & S_2\Delta_2' \end{array}\right] + \left[\begin{array}{c|c} S_1\Delta_1 & S_1\Delta_1' \\ \hline S_2\Delta_2 & 0 \end{array}\right]\right]$$

Hence, again by the same Proposition 1 of Part 2 we conclude that the sensitivity of approximating the column space of the matrix U_2 increases most.

This example demonstrates that the superiority of the RS, being a consequence of (37), can be completely destroyed when using inaccurate reconstructed state variables. However, when accurate reconstructed state quantities are available, the above analysis shows that the superiority of the RS is maintained. Therefore, in the final part of this discussion we formulate more precise guidelines in selecting either the PI or the ordinary MOESP scheme to estimate the model necessary to reconstruct accurately the state quantities.

Since the PI provides asymptotically unbiased estimates, although possibly sensitive ones, without relying on an *a priori* model estimate, we can evaluate the condition in (37) for the model of fixed order estimated by this scheme. If the singular values, ordered in decreasing magnitude, of the matrices

$$\frac{1}{\sqrt{N}} \hat{\Gamma}_i \hat{X}_{1,N} \quad \text{and} \quad \frac{1}{N} \hat{\Gamma}_i \hat{X}_{i+1,i,N} U_{1,i,N}^T \tag{41}$$

are such that those with the same index have the same order of magnitude, the superiority of the RS over the PI scheme does not hold for the estimated model. This is a possible indication that this estimated model may supply accurate reconstructed state quantities to the RS scheme. Whether this actually holds has to be verified explicitly by performing the calculations. The evaluation of the accuracy of the model and the order selection can both be based on the singular values calculated in the different schemes. This is demonstrated in more detail in the simulation study, see Experiment 3 in § 6.2.

If the corresponding singular values of the matrices calculated in (41) differ by an order of magnitude, we have an indication that the condition in (37) holds for the estimated model. When this is the case, the strength of the perturbations v_k becomes an issue. Let $\sigma_{\min}(\cdot)$ denote the smallest singular value of the matrix $(\cdot)$; then, under the condition that

$$\|\Delta_{\text{PI}}\| \approx \sigma_{\min}(\sigma_u^2 \Gamma_i \Delta_i \Delta_i^T \Gamma_i^T) \tag{42}$$

the PI scheme will provide bad estimates of the model corresponding to the small singular values. As a consequence, see (40), the RS scheme will also be sensitive when using this model estimate to provide estimated state quantities. On the other hand, we could simply use the 'biased' model derived from the ordinary MOESP scheme to reconstruct the state quantities. Part of the latter will be badly reconstructed if

$$\|V_{1,i,N}\| \approx \sigma_{\min}(\Gamma_i X_{1,N}) \tag{43}$$

Hence, in that case these poorly reconstructed state quantities increase the sensitivity of certain parts of the model calculated with the RS scheme. The conditions in (42) and (43) are reflected by a small gap between the n largest singular values and the remaining ones of the matrix $R_{22}Q_2U_{1,i,N}^{\mathrm{T}}/N$ in the PI scheme and the matrix R_{22} in the ordinary MOESP scheme respectively. We again refer to the simulation study in § 6 for an illustration of the operation of the presented schemes under such circumstances.

The discussion in the previous paragraph highlights that there is a trade-off in deciding which of the two schemes to use in estimating an *a priori* model necessary in the RS scheme. Although the relevant singular values may give useful information in deciding which *a priori* estimated model to use in the RS scheme, the final answer is obtained by explicitly performing the calculations.

When a more accurate model estimate is obtained, we might iterate further each time using the reconstructed state sequence derived from the previously calculated model. However, at this stage we should bear in mind the insight given by the example after (40), that badly reconstructed modes will not be recovered.

The highlighted condition (37) represents a *critical* condition for the schemes presented in this paper. Therefore, to evaluate the usefulness of the strategy, we have included the example in § 6.2 in the simulation study.

6. Simulation study

In this section, we report the results of two simulation studies to validate the insights obtained in the previous section. Realistic mathematical models are used in both studies. In the first study, an example is analysed representing a non-critical plant as outlined above, while in the second study a critical one is taken. Similar to § 5, the numerical calculations have been performed with the MATLAB package (Moler *et al.* 1987).

6.1. *Identification of a flexible mechanical system*

In the previous section, identification problems were indicated to be non-critical in the identification framework presented in this paper when the deterministic plant $\boldsymbol{P}$ does not give rise to the condition in (37). One such example is analysed in more detail in this section.

6.1.1. *The mathematical model.* The system considered is a discrete-time model of a laboratory set-up. The set-up consists of two circular plates rotated by an electrical servomotor via a flexible shaft. We refer to Hakvoort (1990) for a detailed description of this laboratory experiment. The model of the plant $\boldsymbol{P}$ is given in transfer function form as

$$P(z) = \frac{10^{-3}(0{\cdot}98z^4 + 12{\cdot}99z^3 + 18{\cdot}59z^2 + 3{\cdot}30z - 0{\cdot}02)}{z^5 - 4{\cdot}4z^4 + 8{\cdot}09z^3 - 7{\cdot}83z^2 + 4z - 0{\cdot}86} \tag{44}$$

The output, i.e. the angular rotation of one of the plates, is assumed to be perturbed by a zero-mean white noise sequence filtered by the linear filter F_n as depicted in Fig. 1. The transfer function of this filter has been chosen arbitrarily to be equal to (Schrama 1991)

$$F_n(z) = \frac{0{\cdot}01(2{\cdot}89z^2 + 11{\cdot}13z + 2{\cdot}74)}{z^3 - 2{\cdot}7z^2 + 2{\cdot}61z - 0{\cdot}9}$$

The input sequence $\{u(k)\}$ and the sequence $\{w_1(k)\}$ in Fig. 1 are chosen to be independent zero-mean white noise sequences with variance equal to 1 and 1/9, respectively.

6.1.2. *Experiment 1.* We set up a Monte Carlo simulation study. In each run, a different realization of the output sequence $\{z(k)\}$ is generated while keeping the input sequence $\{u(k)\}$ fixed. The length of the observations is 1200. A total number of 20 runs are made. Each model estimate is evaluated by comparing its Bode plot with the true one. In Figs 2–4, we indicate the latter by the dashed (– – –) lines. These are almost invisible, reflecting the unbiasedness of the obtained estimates.

In this experiment, we evaluate three different scenarios to estimate a model from the input–output data. First, the PI scheme is used. The corresponding information flow is

$$\{u(k), z(k)\} \rightarrow \boxed{\text{PI } i = 20} \rightarrow \text{5th order model} \tag{45}$$

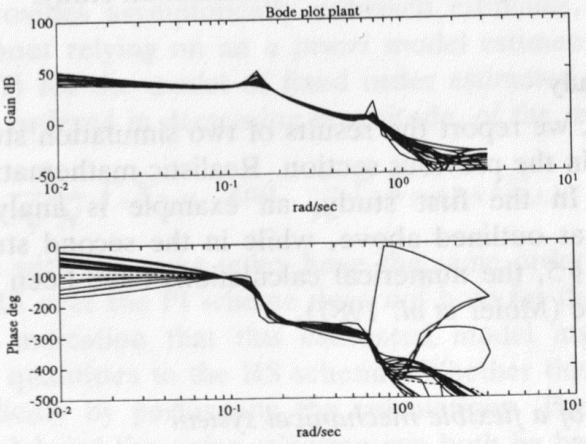

Figure 2. Bode plot of the flexible mechanical system (– – –), and the estimated ones determined by the PI scheme.

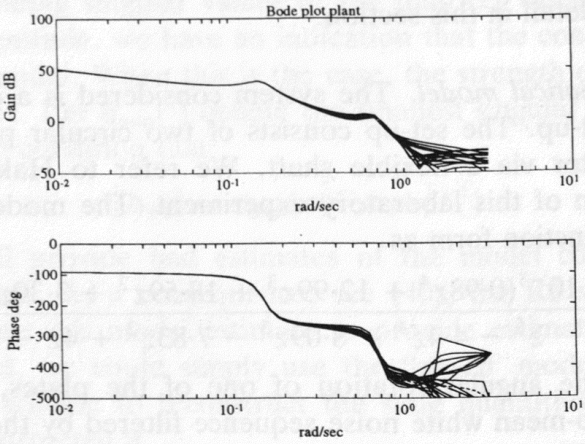

Figure 3. Bode plot of the flexible mechanical system (– – –), and the estimated ones determined by the RS scheme using the true state quantities as instrumental variables.

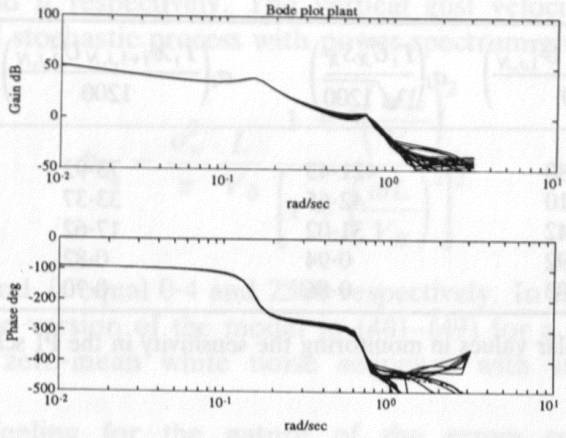

Figure 4. Bode plot of the flexible mechanical system (– – –) and the estimated ones determined by the RS scheme using the reconstructed state quantities based on the model derived by the PI scheme as instrumental variables.

The estimated Bode plots are shown in Fig. 2. Second, the RS scheme is used with the true state quantities taken as instrumental variables. Let $\{x(k)\}_{\text{Eq.(44)}}$, denote the state vector sequence obtained from the model obtained or given in (44), then the information flow is

$$\{u(k),\, z(k)\},\, \{x\{k\}_{\text{Eq.(44)}} \rightarrow \boxed{\text{RS } i = 20,\ \#\text{ iteration} = 0} \rightarrow \text{5th order model} \tag{46}$$

with estimated Bode plots shown in Fig. 3. Third, the RS scheme is used with reconstructed state quantities derived from the model obtained with the PI scheme. The information flow is now

$$\{u(k),\, z(k)\},\, \{x\{k\}_{\text{Eq.(45)}} \rightarrow \boxed{\text{RS } i = 20,\ \#\text{ iteration} = 0} \rightarrow \text{5th order model} \tag{47}$$

With estimated Bode plots shown in Fig. 4.

6.1.3. *Discussion.* To decide whether the underlying input–output data represents a 'critical' system/problem for the class of schemes presented in this paper, we evaluate, as suggested in § 5.4, the condition in (37) for the model estimated with the PI scheme, see (45). The singular values of the different matrices obtained with one particular model estimate are displayed in the first two columns of Table 1. The results obtained with the other model estimates were completely similar. These quantities are compared with the corresponding ones derived from the true model. The latter are displayed in the last two columns of Table 1.

Both the estimated (indicated by the hat) and the true singular values reveal that the condition in (37) does not hold. Therefore, we can use this model with some confidence to reconstruct the state quantities used by the RS scheme. In order to verify this, the experiment indicated in (47) is performed. Comparing Figs 2 and 4, we indeed see that improved estimates result. Based on a single estimate, one observes for the model obtained by (47) that: (1) the five largest singular values in this case increase; and (2) that the norm of the residuals, that

i	$\sigma_i\left(\frac{\Gamma_i \widehat{X_{i+1,i,N}} U_{1,i,N}^{\mathrm{T}}}{1200}\right)$	$\sigma_i\left(\frac{\Gamma_i \widehat{U_X} S_X}{\sqrt{1200}}\right)$	$\sigma_i\left(\frac{\Gamma_i X_{i+1,i,N} U_{1,i,N}^{\mathrm{T}}}{1200}\right)$	$\sigma_i\left(\frac{\Gamma_i U_X S_X}{\sqrt{1200}}\right)$
1	160·80	421·43	73·93	275·48
2	35·10	42·65	33·37	41·73
3	23·42	31·02	17·62	30·19
4	0·92	0·94	0·82	0·85
5	0·83	0·86	0·70	0·75

Table 1. Key singular values in monitoring the sensitivity in the PI scheme in Experiment 1.

is the difference between the measured output and the one obtained on the basis of the estimated model, decreases. A final check, only relevant in a simulation context, is to compare the obtained estimates with those produced in the most favourable case; that is, using the RS with the true state vector sequence. These results are given in Fig. 3. A comparison of this figure with Fig. 2 confirms the insight derived from the condition in (37). Comparing Figs 3 and 4, we observe that the estimates in both cases are of the same accuracy. Therefore, the superiority of the RS scheme holds for this example when using reconstructed state quantities.

6.2. *Identification of the aircraft dynamics when flying through gusty wind*

Critical plants in the framework developed in § 5.4 are those that give rise to the condition in (37) in combination with significant (as stated in (42) and/or (43)) zero-mean but coloured perturbations. An example of such a system is analysed in more detail in this section.

6.2.1. *The mathematical model.* The particular aircraft analysed in this experiment is an F-8 aircraft and the numerical data describing its dynamics is taken from Elliott (1977). The continuous-time model that describes the linearized longitudinal motion of the aircraft hit by a vertical gusty wind at an altitude of 20 000 ft, an airspeed of 620 ft s^{-1} and an angle of attack $\alpha_0 = 0{\cdot}078$ rad is

$$\frac{\mathrm{d}}{\mathrm{d}t}\begin{bmatrix} q \\ u \\ \alpha \\ \theta \end{bmatrix} = \begin{bmatrix} -0{\cdot}49 & 0{\cdot}00005 & -4{\cdot}8 & 0 \\ 0 & -0{\cdot}015 & -14{\cdot}0 & -32{\cdot}2 \\ 1{\cdot}0 & -0{\cdot}00019 & -0{\cdot}84 & 0 \\ 1{\cdot}0 & 0 & 0 & 0 \end{bmatrix} \begin{bmatrix} q \\ u \\ \alpha \\ \theta \end{bmatrix} + \begin{bmatrix} -8{\cdot}7 \\ -1{\cdot}1 \\ -0{\cdot}11 \\ 0 \end{bmatrix} \delta_{\mathrm{e}} + \begin{bmatrix} -4{\cdot}8 \\ -14{\cdot}0 \\ -0{\cdot}84 \\ 0 \end{bmatrix} \alpha_{\mathrm{g}} \tag{48}$$

Here q is the rate of pitch, u the horizontal component of the airspeed, α the angle of attack, θ the pitch angle, δ_{e} the measured elevator deflection angle (deterministic) and α_{g} the unmeasurable scaled vertical gust velocity. Zero-mean white noise with standard deviations equal to 0·05 and 0·2 affect the output

measurements q and u respectively. The vertical gust velocity is a zero-mean normally distributed stochastic process with power spectrum given by

$$\Phi_{\alpha_g} = \frac{\sigma_w^2}{\pi} \frac{L}{V_0} \frac{1 + 3\left(\frac{\omega L}{V_0}\right)^2}{\left[1 + \left(\frac{\omega L}{V_0}\right)^2\right]^2} \tag{49}$$

The quantities σ_w and L equal 0·4 and 2500 respectively. In the simulation, use is made of a discrete version of the model in (48)–(49) for a discrete period of $\Delta t = 0{\cdot}05$ s and a zero-mean white noise sequence with standard deviation $\sigma_\delta = 0{\cdot}1$ for the δ_e.

To get some feeling for the nature of the errors considered in this experiment, we first calculated the auto-correlation functions of the two different components in the total error signal $v(k) + v_z(k)$ in Fig. 1 on the output. These auto-correlation functions indicate strongly correlated stochastic processes. Second, we calculated the signal-to-noise ratio for the individual output quantities. When the signal-to-noise ratio is expressed (in decibels) as $20 \log_{10} \|y\|/\|\tilde{z} - y\|$, then it is approximately 10 dB for the first quantity and 1 dB for the second.

6.2.2. *Experiment 2.* We again set up a Monte Carlo simulation study. Similar to the previous experiment, only one realization of the input $u(k)$ was used and the length of the data sequences was equal to 1200. A total number of 50 runs was performed. From the estimated discrete time models we compute and display the eigenvalues of the transition matrix $\hat{A}_T$.

Now we focus on four different scenarios to produce a model estimate. The scenarios, represented by an information flow diagram are:

$$\{u(k), \tilde{z}(k)\} \rightarrow \boxed{\text{Ordinary MOESP } i = 20} \rightarrow \text{4th order model} \tag{50}$$

The poles of the estimated models are depicted in Fig. 5 on the left-hand side (LHS). The singular values of the matrix $R_{22} \in R^{40\times 40}$, are depicted on the right-hand side (RHS).

$$\{u(k), \tilde{z}(k)\} \rightarrow \boxed{\text{PI } i = 20} \rightarrow \text{4th order model} \tag{51}$$

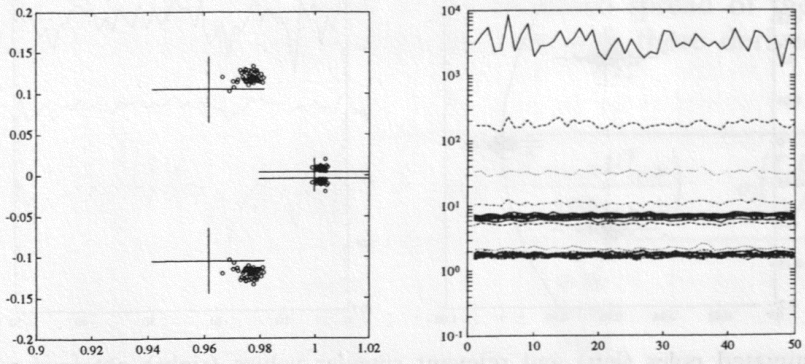

Figure 5. Estimated poles and relevant singular values obtained with the ordinary MOESP scheme.

The poles of the estimated models are depicted in Fig. 6 on the LHS. The singular values of interest now are those of the matrix $R_{22}R_{32}^{\mathrm{T}} \in R^{40\times 20}$. They are plotted on the RHS.

$$\{u(k), \tilde{z}(k)\}, \{x(k)\}_{\text{Eq.(50)}} \rightarrow \boxed{\text{RS } i = 20, \text{ \# iteration} = 0} \rightarrow \text{4th order model} \tag{52}$$

The poles of the estimated models are depicted in Fig. 7 on the LHS. The singular of the matrix $R_{22}R_{32}^{\mathrm{T}} \in R^{40\times 4}$ are plotted on the RHS.

$$\{u(k), \tilde{z}(k)\}, \{x(k)\}_{\text{Eq.(51)}} \rightarrow \boxed{\text{RS } i = 20, \text{ \# iteration} = 8} \rightarrow \text{4th order model} \tag{53}$$

The poles of the estimated models and the relevant singular values are depicted on the LHS, respectively the RHS, of Fig. 8.

6.2.3. *Discussion.* Similar to the previous experiment, we present the results of one arbitrarily selected model, estimated as specified in (51), to evaluate the condition in (37). The relevant singular values are now displayed in Table 2. In the first two columns are those values corresponding to the estimated model; in the last two columns, those derived from the true model. The estimated

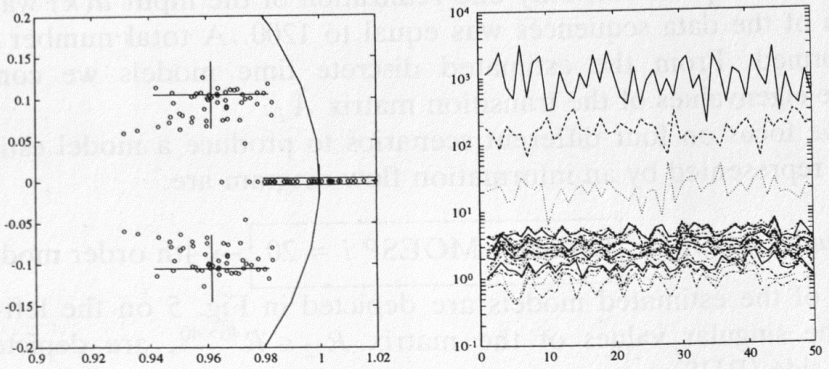

Figure 6. Estimated poles (left) and relevant singular values (right) obtained with the PI scheme.

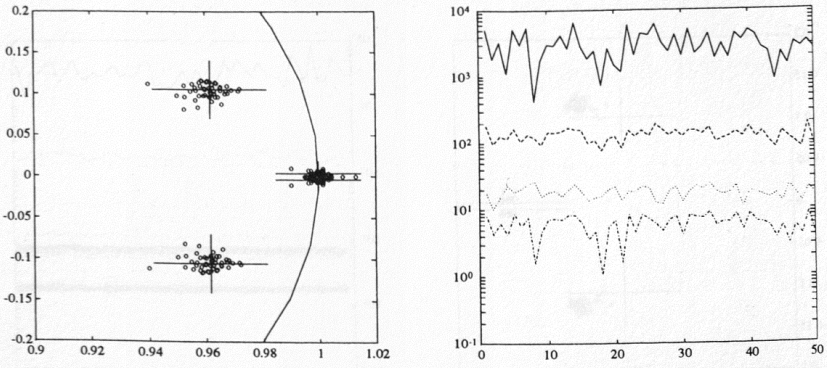

Figure 7. Estimated poles (left) and relevant singular values (right) obtained with the RS scheme using the reconstructed state quantities based on the model derived by the ordinary MOESP scheme.

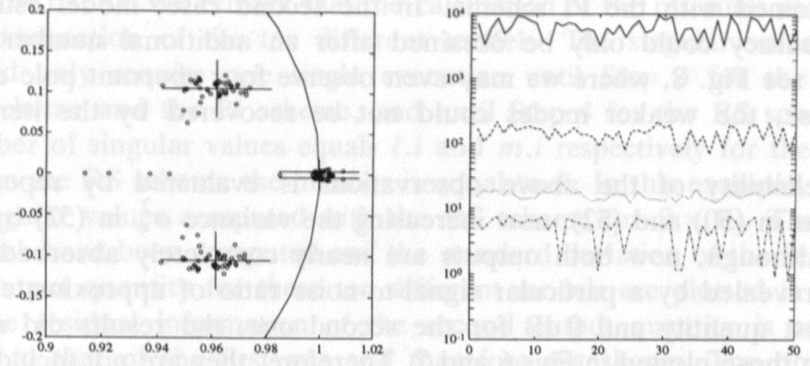

Figure 8. Estimated poles (left) and relevant singular values (right) obtained with the RS scheme using the reconstructed state quantities based on the model derived by the PI scheme as instrumental variables and eight iterations.

quantities in columns 1 and 2 of Table 2 clearly differ by an order of magnitude. The true quantities in columns 3 and 4 confirm this observation. Therefore, this observation stresses the fact that although the computations within the PI are quite sensitive in the present case, as shown in Fig. 6, the estimated model provides useful information on the condition in (37).

The suggested route to follow in the identification process was *first* to inspect the singular values of the matrix $R_{22}Q_2U_{1,i,N}^{\mathrm{T}}$ in the PI scheme and those of the matrix R_{22} in the ordinary MOESP scheme. In the first case, see Fig. 6 on the right-hand side for a particular run, we clearly observe that the fourth singular value is buried in the noise. Therefore, the corresponding part of the state-space model will be poorly identified. This is confirmed in the right-hand side of this figure. In the second case, see Fig. 5 on the right-hand side for a particular run, we observe that although the perturbations are quite strong, there is a small gap between the fourth singular value and the next smaller ones. This suggests that the increased numerical robustness in combination with the biasedness of the model estimated with the ordinary MOESP scheme is preferred over the unbiased but sensitive calculations with the PI scheme.

Second, to check whether this is indeed the right decision, we evaluate the models estimated with the RS scheme using the model estimated by the ordinary MOESP scheme, respectively the PI scheme, as *a priori* models. In the first case, (52), we observe that the bias of the model is indeed removed and that the increased sensitivity of the estimates or the increased spread of the estimated poles, is limited and much smaller than the case with those derived from the

i	$\sigma_i\left(\frac{\Gamma_i X_{i+1,i,N} U_{1,i,N}^{\mathrm{T}}}{1200}\right)$	$\sigma_i\left(\frac{\Gamma_i \widehat{U_X} S_X}{\sqrt{1200}}\right)$	$\sigma_i\left(\frac{\Gamma_i X_{i+1,i,N} U_{1,i,N}^{\mathrm{T}}}{1200}\right)$	$\sigma_i\left(\frac{\Gamma_i U_X S_X}{\sqrt{1200}}\right)$
1	1·95	68·76	4·38	204·62
2	0·076	1·82	0·063	3·59
3	0·018	0·46	0·022	0·52
4	0·0007	0·008	0·0007	0·2

Table 2. Key singular values in monitoring the sensitivity in the PI scheme in Experiment 2.

model obtained with the PI scheme. In the second case, model estimates of similar accuracy could only be obtained after an additional number of eight iterations, see Fig. 8, where we may even observe four aberrant pole estimates. In this case, the weaker modes could not be recovered by the iterative RS scheme.

The reliability of the above observations is evaluated by repeating the calculations in (50) and (52), now increasing the variance σ_w^2 in (52) by a factor of five. Although, now both outputs are nearly completely absorbed into the noise, as revealed by a particular signal-to-noise ratio of approximately -7 dB for the first quantity and 0 dB for the second one, the results did not differ much from those plotted in Figs 6 and 7. Therefore, they are not included in the present paper for the sake of brevity, and we restrict mentioning that the estimates obtained as outlined in (50) showed an increased bias, while those obtained as outlined in (52) again became unbiased with a marginal increase in spread compared with Fig. 7. This reliability of the combined ordinary MOESP/RS scheme to identify 'critical' plants was also demonstrated in other simulation examples, such as reported by Verhaegen and Lycklame á Nyeholt (1990).

6.2.4. *Experiment 3.* In the previous two experiments, models of fixed order were estimated. In addition, we occasionally evaluated the accuracy of the obtained model estimates by inspecting the spread of the estimated quantities under consideration (Bode plots or poles) around the true quantity. In a realistic identification problem, neither the order of the deterministic plant nor more than one input–output data pair are generally available. Therefore, we evaluate in this final experiment how the presented schemes and insights can be used to supply this information. We take the critical plant used in Experiment 2 as a test vehicle.

Two measures are considered for this purpose. A first set of measures are the singular values computed in the different MOESP schemes of this paper. When $i > n$ and the input $u(k)$ is suitably chosen, the order of the system corresponds to the number of non-zero singular values in the error-free case. Therefore, as remarked in the paragraph following Theorem 1 of Part 2 (Verhaegen and Dewilde 1992 b), the decision on the order boils down to dividing the singular values into 'significant' ones and 'neglectable' ones. This division becomes easy when there is a clear gap between these two groups of singular values. As pointed out in the discussion in § 5.4, such a clear gap is also a qualitative measure that the sensitivity of approximating the column space of the matrix Γ_i is low. Therefore, the singular values alone can be used both to decide on the model order as well as to judge the accuracy of the calculations. However, in order to support this decision, it is proposed to use a second measure, namely the norm of the one-step prediction error (Ljung 1987). For the output-error type of models, these are simply the residuals; that is, the difference between the measured output and the reconstructed output based on the estimated model. This second measure is, however, not relevant in the computations.

These two measures are now calculated for the example discussed in Experiment 2 for the three different schemes analysed in this paper. Using a single time sequence of the input–output pair $\{u(k), \tilde{z}(k)\}$ we identify models

of order $\hat{n} = 1{:}1{:}10$. We remark that the calculation of the residuals requires the explicit computation of the ten different models. The singular values on the other hand only require one single execution until Step 3 for the ordinary MOESP scheme and the PI scheme, and until Step 4 for the RS scheme. The total number of singular values equals $l.i$ and $m.i$ respectively for the first two schemes; in the RS scheme the number is equal to $\hat{n}$. In this example, we focus on the singular values computed with the RS scheme for $\hat{n} = 10$. The singular values which have been computed and the standard deviation of the residuals of the first output quantity for these ten different models are plotted in our final figure. The residual information of the second output quantity is completely analogous to that of the first one and therefore not shown. The objective in selecting a system of order $\hat{n}$ is to find a big gap between the $\hat{n}$th and the $\hat{n}+1$th singular value, while the residual of the $\hat{n}$th order systems is (close to) the minimal one. With the information derived by the ordinary MOESP scheme (see Fig 9(a)) the selection of order one or four would then be plausible. From that derived by the PI scheme (see Fig. 9(b)) a third order system is suggested. The standard deviation of the residuals of the first and second-order system fall outside the range of the figure. The clearest decision on the order, which happened to be the correct one, is obtained from the information supplied by the RS scheme. Note that this model also has the smallest standard deviation of the residuals compared with the models of order 4 obtained with the other two schemes.

In order to verify that the last observation did not depend on the particular input–output data batch used, we performed a similar Monte Carlo simulation study of 50 runs as reported in Experiment 2. In 95% of the cases, the ordered singular values computed with the RS scheme for $\hat{n} = 10$ showed a clear gap between the 4th and 5th singular value, similar to the one in Fig. 9(c). In the other marginal cases, a gap as in Fig. 9(a) resulted. However, even in these cases, the minimal residual would still highlight the correct system order. For the sake of brevity, these results are not shown in this paper.

7. Conclusions

The 'subspace model identification' (SMI) class of algorithms presented in this series of papers is formulated and analysed in a linear algebra framework. This way of approaching the linear system identification problem has been demonstrated to lead to a successful analysis of theoretical questions, such as the asymptotic unbiasedness, as well as to contribute to the convenient nature of the derived schemes. In this set of final remarks, we draw special attention to the following convenient aspects.

(i) The algorithmic structure of the numerical schemes, derived for both the basic and the general (open-loop) identification problem, is completely similar, namely an RQ factorization followed by a SVD and finally the solution of overdetermined sets of equations. This common structure of the algorithms is certainly beneficial in implementing these schemes, and would also be an asset when mapping them on a dedicated systolic array. On classical sequential computer architectures, the special attention given to the efficiency of the computations works to the advantage of the use of these schemes.

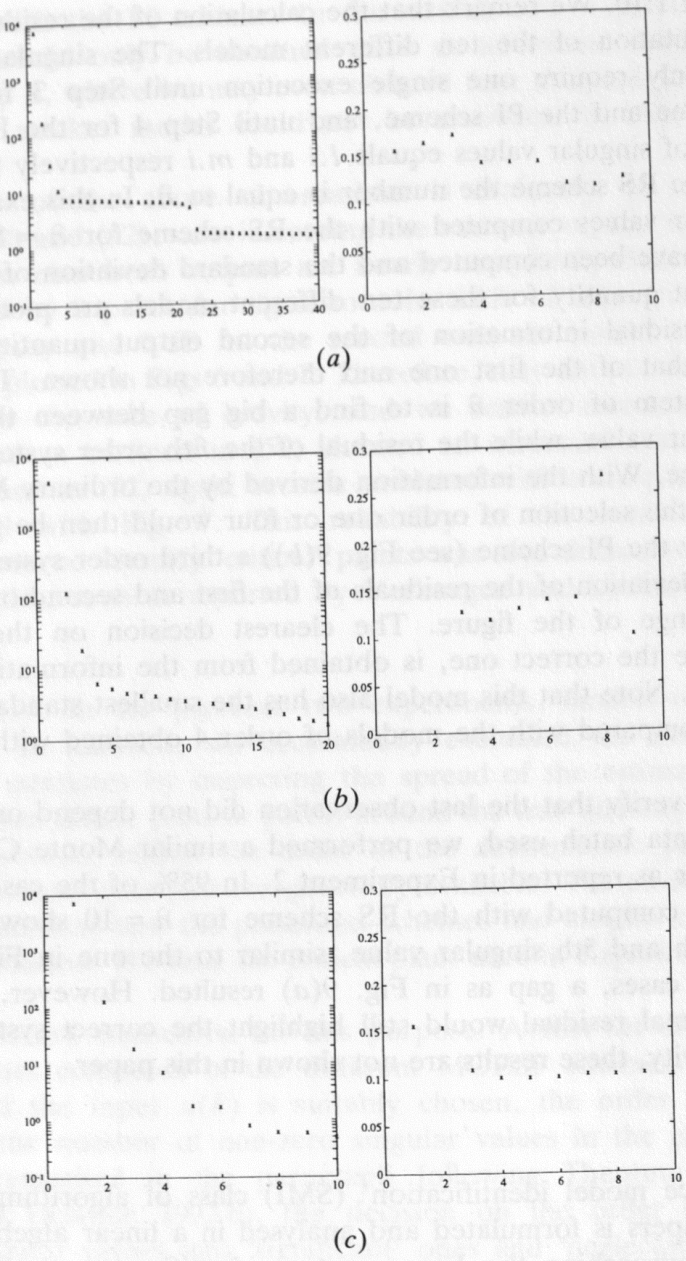

Figure 9. (*a*) Relevant singular values (left) and the standard deviation of the residual on the first output quantity (right) obtained with the ordinary MOESP scheme for model orders 1:10. (*b*) Relevant singular values (left) and the standard deviation of the residual on the first output quantity (right) obtained with the PI scheme for model orders 1:10. (*c*) Relevant singular values (left) and the standard deviation of the residual on the first output quantity (right) obtained with the RS scheme using the reconstructed state quantities based on the model derived by the ordinary MOESP scheme for model orders 1:10.

(ii) Except for the ordinary MOESP scheme extended with instrumental variables based on reconstructed state quantities, indicated by the RS scheme, the schemes presented in this series of papers require the tuning of only two parameters, irrespective of multiple inputs or outputs. These two parameters are first the dimension parameter i, determining the

(row) size of the data Hankel matrices processed by the different schemes and, second, the order of the system. This reduced number of parameters enables easy visualization of an accuracy measure, such as the norm of the residuals on the output quantity.

(iii) The singular values can supply very useful information in making a motivated choice on the two tuning parameters indicated in item (ii). The selection of both correspond to the detection of a clear gap in the ordered singular values. In addition, it has been shown that such a gap is also a qualitative measure for the accuracy of the obtained estimates. Therefore, a detailed sensitivity analysis is performed that *a priori* highlights the schemes that will lead to the largest relevant gap. The latter schemes are those that implicitly approximate the controllability gramian accurately. When the input quantity is chosen as zero-mean white noise, two schemes closely approximate this gramian, i.e. the MOESP2 and the RS scheme, irrespective of the choice of the dimension parameter i (as long as it is chosen larger than the system order). For the other schemes, the same reliability is achieved by choosing an extremely large dimension parameter i. Among other things, this affects the computational efficiency in a very undesirable way, as was mentioned in the concluding remarks of Part 2 (Verhaegen and Dewilde 1992 b). We remark that the increased reliability of the RS scheme depends on the accurate reconstruction of the state sequence of the deterministic part of the system. Again, here the singular values of the different schemes enabled the set up of a strategy to make the best *a priori* model choice for this purpose.

Although, this final paper has addressed and solved a realistic open-loop identification problem, not every aspect of the schemes presented has yet been fully understood, such as which class of systems or identification problems cannot be handled by the proposed schemes. Some preliminary insight in this matter can be obtained from the sensitivity analysis presented in this paper, i.e. for critical plants with strong and highly coloured perturbations on the output. The experimental analysis has shown that the RS scheme can be very robust even for such systems. However, we may expect extreme difficulties for systems of large order which, in the error-free case, show a gradual decay in the singular values. Further research on this topic is required. Additional items for further research are the following.

(i) The qualitative information on the accuracy of the obtained information can be very useful in a preliminary analysis of an identification problem. However, in a number of applications more detailed quantitative (covariance) information is required. For the ordinary MOESP scheme, an initial analysis is made in Viberg *et al.* (1991) to derive covariance information about the poles estimated from the system matrix. This analysis has to be extended to more general estimates, such as uncertainty levels of Bode plots, and to the other algorithmic variants presented in this series.

(ii) A comparative study of the presented approach, both on a theoretical level and on an experimental level, has to be made with other SMI

schemes. In Part 2 (Verhaegen and Dewilde 1992 b), a comparison has been made with the classical Ho, Kalman-based approach described by Kung (1978). However, other recently proposed strategies should be included in such a study, e.g. Moonen *et al.* (1989) and Larimore (1990). Furthermore, the relationship and complementarity to the parametric model identification strategies, developed by Söderström and Stoica (1989), Ljung (1987), should be further strengthened.

(iii) The identification problems addressed in this series of papers require open-loop experiments. An extension to an application of the developed strategies to closed-loop experiments is highly desired. We refer the interested reader to Verhaegen (1993) for a possible solution to such problems.

(iv) As highlighted in Experiment 2, the sensitivity of the calculations to the perturbations on the data increases when all the dominant poles are close to the unit circle. Changing the sample rate might be a possible cure to decreasing the sensitivity. However, a more rigorous method of improving the estimates might be through the derivation of the schemes presented in this series of papers in the δ-operator framework as developed by Middleton and Goodwin (1990).

Acknowledgment

The research of Dr Michel Verhaegen has been made possible by a fellowship from the Royal Dutch Academy of Arts and Sciences. The author thanks Professor Bart De Moor and researcher Peter Van Overschee, both from the Catholic University of Leuven in Belgium, for discussions on the instrumental variable approach based on past input measurements.

Appendix A

Proof of Theorem 1: From (4) we obtain

$$U_{1,i,N} = R_{11}^N Q_1^N \tag{54}$$

Further, introduce the data equation (1)

$$Z_{1,i,N} = R_{21}^N Q_1^N + R_{22}^N Q_2^N = \Gamma_i X_{1,N} + H_i U_{1,i,N} + V_{1,i,N} \tag{55}$$

From (5) we obtain

$$X_{1,N} = R_{x1} Q_1^N + R_{x2}^N Q_2^N \tag{56}$$

Substitution of (56), (54) into (55) yields

$$\Gamma_i R_{x1} Q_1^N + \Gamma_i R_{x2}^N Q_x^N + H_i R_{11}^N Q_1^N + V_{1,i,N} = R_{21}^N Q_1^N + R_{22}^N Q_2^N \tag{57}$$

From (9) and (54) we obtain

$$\frac{1}{\sqrt{N}} V_{1,i,N} (Q_1^N)^{\mathrm{T}} \frac{1}{\sqrt{N}} (R_{11}^N)^{\mathrm{T}} = \varepsilon_N^6 E_N^6$$

Since condition (28) of Part 1 (Verhaegen and Dewilde 1992 a) is fulfilled, there exists an $\bar{N}$ such that for $N > \bar{N}$, the square matrix R_{11}^N is non-singular, hence

$$\frac{1}{\sqrt{N}} V_{1,i,N}(Q_1^N)^T = \varepsilon_N^6 E_N^6 \left(\frac{1}{\sqrt{N}} (R_{11}^N)^T\right)^{-1} \tag{58}$$

Using this relationship and the facts that $Q_x^N(Q_1^N)^T = Q_2^N(Q_1^N)^T = 0$ and $Q_1^N(Q_1^N)^T = I_{m.i}$, (57) after multiplication on the right with $(Q_1^N)^T/\sqrt{N}$ becomes

$$\frac{1}{\sqrt{N}} \Gamma_i R_{x1} + \frac{1}{\sqrt{N}} H_i R_{11}^N + \varepsilon_N^6 E_N^6 \left(\frac{1}{\sqrt{N}} (R_{11}^N)^T\right)^{-1} = \frac{1}{\sqrt{N}} R_{21}^N$$

Hence

$$\frac{1}{\sqrt{N}} (\Gamma_i R_{x1} + H_i R_{11}^N - R_{21}^N) = -\varepsilon_N^6 E_N^6 \left(\frac{1}{\sqrt{N}} (R_{11}^N)^T\right)^{-1}$$

and (57) becomes

$$\frac{1}{\sqrt{N}} R_{22}^N Q_2^N = -\varepsilon_N^6 E_N^6 \left(\frac{1}{\sqrt{N}} (R_{11}^N)^T\right)^{-1} Q_1^N + \frac{1}{\sqrt{N}} \Gamma_i R_{x2}^N Q_x^N + \frac{1}{\sqrt{N}} V_{1,i,N} \tag{59}$$

Using (58) and the fact that $Q_x^N(Q_1^N)^T = 0$, $1/N R_{22}^N (R_{22}^N)^T$ becomes

$$\begin{aligned}
\frac{1}{N} R_{22}^N (R_{22}^N)^T &= \frac{1}{N} \Gamma_i R_{x2}^N (R_{x2}^N)^T \Gamma_i^T + \frac{1}{N} \Gamma_i R_{x2}^N Q_x^N V_{1,i,N}^T + \frac{1}{N} V_{1,i,N} V_{1,i,N}^T \\
&\quad + \frac{1}{N} V_{1,i,N}(Q_x^N)^T (R_{x2}^N)^T \Gamma_i^T \\
&\quad - \frac{1}{\sqrt{N}} V_{1,i,N}(Q_1^N)^T \left(\frac{1}{\sqrt{N}} (R_{11}^N)\right)^{-1} \varepsilon_N^6 (E_N^6)^T \\
&\quad + \varepsilon_N^6 E_N^6 \left(\frac{1}{\sqrt{N}} (R_{11}^N)^T\right)^{-1} (R_{11}^N)^{-1} \varepsilon_N^6 (E_N^6)^T \\
&\quad - \varepsilon_N^6 E_N^6 \left(\frac{1}{\sqrt{N}} (R_{11}^N)^T\right)^{-1} Q_1^N \frac{1}{\sqrt{N}} V_{1,i,N}^T \\
&= \frac{1}{N} \Gamma_i R_{x2}^N (R_{x2}^N)^T \Gamma_i^T + \underbrace{\frac{1}{N} \Gamma_i R_{x2}^N Q_x^N V_{1,i,N}^T} + \frac{1}{N} V_{1,i,N} V_{1,i,N}^T \\
&\quad + \frac{1}{N} V_{1,i,N}(Q_x^N)^T (R_{x2}^n)^T \Gamma_i^T \\
&\quad - \varepsilon_N^6 E_N^6 \left(\frac{1}{N} R_{11}^N (R_{11}^N)^T\right)^{-1} \varepsilon_N^6 (E_N^6)^T
\end{aligned} \tag{60}$$

We now turn to the underbraced term in the above expression. From (10) and (56) we deduce

$$\frac{1}{N} R_{x1}^N Q_1^N V_{1,i,N}^T + \frac{1}{N} R_{x2}^N Q_x^N V_{1,i,N}^T = \varepsilon_N^7 E_N^7$$

With (58) this equality becomes

$$\left(\frac{1}{\sqrt{N}}\,R_{x1}^N\right)\left(\frac{1}{\sqrt{N}}\,(R_{11}^N)\right)^{-1}\varepsilon_N^6(E_N^6)^{\mathrm{T}}+\frac{1}{N}\,R_{x2}^N Q_x^N V_{1,i,N}^{\mathrm{T}}=\varepsilon_N^7 E_N^7$$

Since the limits in (6) and (8) exist, the limits of the different factors, namely

$$\lim_{N\to\infty}\left(\frac{1}{\sqrt{N}}\,R_{x1}^N\right)\quad\text{and}\quad\lim_{N\to\infty}\left(\frac{1}{\sqrt{N}}\,(R_{11}^N)\right)$$

also exist (up to an orthogonal right transformation) and therefore, the matrix multiplication

$$\left(\frac{1}{\sqrt{N}}\,R_{x1}^N\right)\left(\frac{1}{\sqrt{N}}\,(R_{11}^N)^{\mathrm{T}}\right)^{-1}$$

exists in the limit $N\to\infty$. Hence, we can define a new sequence of real numbers ε_N^8 and bounded matrices E_N^8 such that

$$\frac{1}{N}\,R_{x2}^N Q_x^N V_{1,i,N}^{\mathrm{T}}=\varepsilon_N^8 E_N^8$$

With this expression for the underbraced term in (60), the latter equation becomes

$$\begin{aligned}\frac{1}{N}\,R_{22}^N(R_{22}^N)^{\mathrm{T}}&=\frac{1}{N}\,\Gamma_i R_{x2}^N(R_{x2}^N)^{\mathrm{T}}\Gamma_i^{\mathrm{T}}+\frac{1}{N}\,V_{1,i,N}V_{1,i,N}^{\mathrm{T}}\\&\quad+\Gamma_i\varepsilon_N^8E_N^8+\varepsilon_N^8(E_N^8)^{\mathrm{T}}\Gamma_i^{\mathrm{T}}-\varepsilon_N^6E_N^6\left(\frac{1}{N}\,R_{11}^N(R_{11}^N)^{\mathrm{T}}\right)^{-1}\varepsilon_N^6(E_N^6)^{\mathrm{T}}\end{aligned}\tag{61}$$

Taking the limit $N\to\infty$ of both sides, we obtain the result of the theorem. □

Appendix B

Proof of Lemma 1: With the state-space representation of the system in the Lemma 1 and using the independence between $u(k)$ and $v(l)$, we can express the limit in Lemma 1 as

$$\lim_{N\to\infty}\frac{1}{N}\sum_{j=1}^{N}\eta_{j+1}v_{j+l-1}^{\mathrm{T}}$$

$$=\lim_{N\to\infty}\frac{1}{N}\sum_{j=1}^{N}\Phi\eta_j v_{j+l-1}^{\mathrm{T}}+\underbrace{\lim_{N\to\infty}\frac{1}{N}\sum_{j=1}^{N}\Gamma u_j v_{j+l-1}^{\mathrm{T}}}_{=0}$$

$$=\lim_{N\to\infty}\left(\frac{1}{N}\,\Phi\eta_1 v_l^{\mathrm{T}}+\frac{1}{N}\sum_{j=2}^{N}\Phi\eta_j v_{j+l-1}^{\mathrm{T}}\right)$$

$$=\lim_{N\to\infty}\left(\frac{1}{N}\,\Phi\eta_1 v_l^{\mathrm{T}}+\frac{1}{N}\sum_{\mu=1}^{N-1}\Phi\eta_{\mu+1}v_{l+\mu}^{\mathrm{T}}+\frac{1}{N}\,\Phi\eta_{N+1}v_{N+l}^{\mathrm{T}}\right)$$

$$= \lim_{N\to\infty}\left(\frac{1}{N}\Phi\eta_1 v_l^{\mathrm{T}} + \frac{1}{N}\sum_{\mu=1}^{N}\Phi^2\eta_\mu v_{l+\mu}^{\mathrm{T}}\right) + \underbrace{\lim_{N\to\infty}\frac{1}{N}\sum_{\mu=1}^{N}\Phi\Gamma u_\mu v_{l+\mu}^{\mathrm{T}}}_{=0}$$

$$\vdots$$

$$= \lim_{N\to\infty}\frac{1}{N}\sum_{s=1}^{N}\Phi^s\eta_1 v_{s+l-1}^{\mathrm{T}}$$

$$= 0$$

The third equality holds since

$$\lim_{N\to\infty}\frac{1}{N}\Phi\eta_{N+1}v_{N+l}^{\mathrm{T}} = 0$$

while the last equality holds since the sequence $[\Phi\eta_1 \quad \Phi^2\eta_1 \quad \dots\ ]$ is a deterministic time sequence and the noise v_l has mean zero. □

References

Elliott, J. R., 1977, NASA's advanced control law program for the F-8 digital fly-by-wire aircraft. *IEEE Transactions on Automatic Control*, **22**, 753–757.

Hakvoort, R., 1990, Approximate identification in the controller design problem. Master's Thesis, Measurement and Control Theory Section. Mechanical Engineering Department, Delft University of Technology, **A-538**.

Kung, S. Y., 1978, A new identification and model reduction algorithm via singular value decomposition. *12th Asilomar Conference on Circuits, Systems and Computers*, pp. 705–714.

Larimore, W., 1990, Canonical Variate Analysis in Identification, Filtering and Adaptive Control. *Proceedings of the 29th Conference on Decision and Control*, pp. 596–604.

Ljung, L., 1987, *System Identification: Theory for the User* (Englewood Cliffs, NJ: Prentice Hall).

Middleton, R. H., and Goodwin, G. C., 1990, *Digital Control and Estimation, a Unified Approach* (Englewood Cliffs, NJ: Prentice Hall)

Moler, C., Little, J., and Bangert, S., 1987, *PRO-MATLAB User's Guide* (Natick, Mass: The MathWorks Inc).

Moonen, M., Moor, B. De, Vandenberghe, L., and Vandewalle, J., 1989, On- and off-line identification of linear state-space models. *International Journal of Control*, **49**, 219–232.

Moonen, M., and Vandewalle, J., 1990, QSVD approach to on- and off-line state space identification. *International Journal of Control*, **50**, 1133–1146.

Paige, C. C., and Saunders, M. A., 1981, Towards a generalized singular value decomposition. *SIAM Journal of Numerical Analysis* **18**, 398–405.

Schrama, R. J. P., 1991, An open-loop solution to the approximate closed-loop identification problem. *Preprints of the 9th IFAC/IFORS Symposium on Identification and System Parameter Estimation*, pp. 1602–1607.

Söderström, T., and Stoica, P., 1989, *System Identification* (Englewood Cliffs, NJ: Prentice Hall).

Verhaegen, M., 1993, Application of a subspace model identification technique to identify LTI systems operating in closed loop. *Automatica*, to be published.

Verhaegen, M., and Dewilde, P., 1992 a, Subspace model identification. Part 1: The output-error state space model identification class of algorithms. *International Journal of Control*, **56**, 1187–1210; 1992 b, Subspace model identification. Part 2: Analysis of the elementary output-error state space model identification algorithm. *Ibid.*, **56**, 1211–1241.

Verhaegen, M., and Lycklama, Á, and Nyeholt, D., 1990, Experimental analysis of a new MIMO state space model identification technique using simulated and real ship data. Technical Report N90.07, Network Theory Section, Delft University of Technology.

VIBERG, M., OTTERSTEN, B., WAHLBERG, B., and LJUNG, L., 1991, A statistical perspective on state-space modeling using subspace methods. *Proceedings of the 30th Conference on Decision and Control*, pp. 1337–1342.